

See discussions, stats, and author profiles for this publication at: <https://www.researchgate.net/publication/51618566>

# Isolation and in vitro expansion of human colonic stem cells

Article in *Nature medicine* · September 2011

DOI: 10.1038/nm.2470 · Source: PubMed

CITATIONS

407

READS

1,011

12 authors, including:



**Peter Jung**

German Cancer Research Center

41 PUBLICATIONS 3,047 CITATIONS

SEE PROFILE



**Toshiro Sato**

Keio University

145 PUBLICATIONS 15,926 CITATIONS

SEE PROFILE



**Mar Iglesias**

Consorci MAR Parc de Salut de Barcelona

137 PUBLICATIONS 4,699 CITATIONS

SEE PROFILE



**David Rossell**

University Pompeu Fabra

53 PUBLICATIONS 3,128 CITATIONS

SEE PROFILE

Some of the authors of this publication are also working on these related projects:



Hypersaline Infusion Protocol through the Portal Vein may Focus Electroporation on Tumor Tissue, but is it really Safe? Preliminary Results [View project](#)



Organoids [View project](#)

# Isolation and *in vitro* expansion of human colonic stem cells

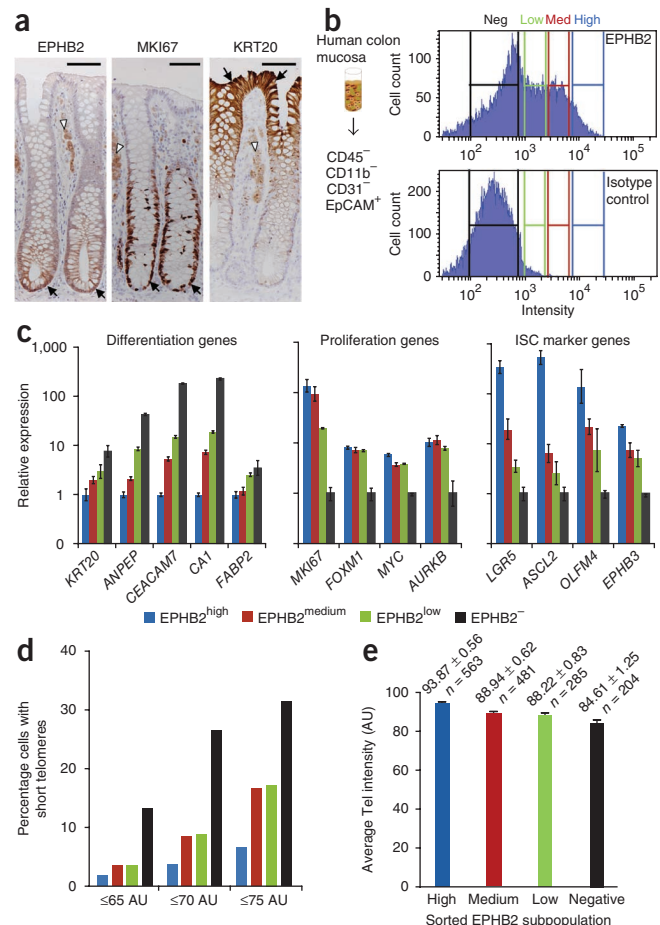
Peter Jung<sup>1,8</sup>, Toshiro Sato<sup>2,3,8</sup>, Anna Merlos-Suárez<sup>1</sup>, Francisco M Barriga<sup>1</sup>, Mar Iglesias<sup>4</sup>, David Rossell<sup>5</sup>, María M Gallardo<sup>6</sup>, María A Blasco<sup>6</sup>, Elena Sancho<sup>1</sup>, Hans Clevers<sup>2</sup> & Eduard Batlle<sup>1,7</sup>

Here we describe the isolation of stem cells of the human colonic epithelium. Differential cell surface abundance of ephrin type-B receptor 2 (EPHB2) allows the purification of different cell types from human colon mucosa biopsies. The highest EPHB2 surface levels correspond to epithelial colonic cells with the longest telomeres and elevated expression of intestinal stem cell (ISC) marker genes. Moreover, using culturing conditions that recreate the ISC niche, a substantial proportion of EPHB2-high cells can be expanded *in vitro* as an undifferentiated and multipotent population.

Throughout the human lifespan, colon stem cells (CoSCs) renew the epithelium that lines the large intestine<sup>1</sup>. It is believed that alterations in the biology of CoSCs account for the pathophysiology of various

**Figure 1** Characterization of epithelial colon cells purified from human mucosa samples according to different EPHB2 surface levels. (a) Immunohistochemistry analysis for EPHB2, proliferation marker MKI67 and pan-differentiation marker KRT20 on serial sections of normal human colonic mucosa obtained from a colectomy sample from a subject with colorectal cancer disease. Scale bars, 50  $\mu$ m. Black arrows indicate specific staining, and white arrowheads indicate nonspecific background staining (see **Supplementary Fig. 1b**). (b) Top, FACS profile of single-cell suspensions from normal human colonic crypts staining with antibody to EPHB2. Nonepithelial cell lineages were identified as CD11b<sup>+</sup>, CD31<sup>+</sup> or CD45<sup>+</sup> and discarded from the analysis. The epithelial marker EpCAM was used to select positively for epithelial cells. Bottom, IgG control staining was performed to define the EPHB2<sup>+</sup> cell population. (c) Quantitative RT-PCR (qRT-PCR) analysis of expression levels of ISC, proliferation or differentiation genes on colon epithelial cells purified by FACS according to different EPHB2 surface levels. Error bars indicate s.d. ( $n = 3$ ). *CEACAM7*, carcinoembryonic antigen-related cell adhesion molecule 7; *FOXM1*, forkhead box M1; *MYC*, Myc oncogene; *AURKB*, aurora kinase B. (d) Percentage of cells with relatively short telomeres as measured by fluorescence *in situ* hybridization (FISH) in each EPHB2-purified cell population. Cells with short telomeres were defined according to three different ranges of average telomere fluorescence arbitrary units (AU); cells with  $\leq 65$  AU,  $\leq 70$  AU or  $\leq 75$  AU according to the quantitative FISH histograms depicted in **Supplementary Figure 2**. (e) Average telomere (Tel) length in EPHB2-sorted colon cell populations. The observed differences in average telomere length are highly significant ( $P < 0.01$ ) except for the EPHB2<sup>medium</sup> to EPHB2<sup>low</sup> comparison ( $P = 0.488$ ). Error bars indicate s.d.

large-bowel disorders, including colorectal cancer<sup>2</sup>. Yet the identification of CoSCs remains elusive. The *EPHB2* gene encodes a receptor tyrosine kinase whose activity in mouse intestine is required to position different cell types along the crypt axis<sup>3</sup>. High amounts of EPHB2 characterize mouse small intestine ISCs as well as colorectal cancer stem cells<sup>4</sup>. In human colon epithelium, EPHB2 cell abundance was maximal at the bottom of crypts and decreased along a gradient as epithelial cells migrated upward (**Fig. 1a** and **Supplementary Fig. 1**). Cells within the crypt proliferation compartment (MKI67<sup>+</sup> domain) had heterogeneous amounts of EPHB2, whereas differentiated cells of the surface epithelium (keratin 20 positive, KRT20<sup>+</sup>) stained negative for EPHB2 (**Fig. 1a** and **Supplementary Fig. 1**). Using an antibody against the extracellular domain of EPHB2, we purified intestinal epithelial cells from normal fresh tissue samples obtained from colectomies of individuals suffering



<sup>1</sup>Oncology program, Institute for Research in Biomedicine, Barcelona, Spain. <sup>2</sup>Hubrecht Institute and University Medical Center Utrecht, Utrecht, The Netherlands. <sup>3</sup>Department of Gastroenterology, School of Medicine, Keio University, Shinjuku-ku, Tokyo, Japan. <sup>4</sup>Department of Pathology, Hospital Universitari del Mar, Universitat Autònoma de Barcelona, Barcelona, Spain. <sup>5</sup>Biostatistics and Bioinformatics Unit, Institute for Research in Biomedicine, Barcelona, Spain. <sup>6</sup>Telomeres and Telomerase Group, Molecular Oncology Program, Spanish National Cancer Research Center, Madrid, Spain. <sup>7</sup>Institució Catalana de Recerca i Estudis Avançats, Barcelona, Spain. <sup>8</sup>These authors contributed equally to this work. Correspondence should be addressed to E.B. (eduard.batlle@irbbarcelona.org).

Received 25 February; accepted 14 August; published online 4 September 2011; doi:10.1038/nm.2470

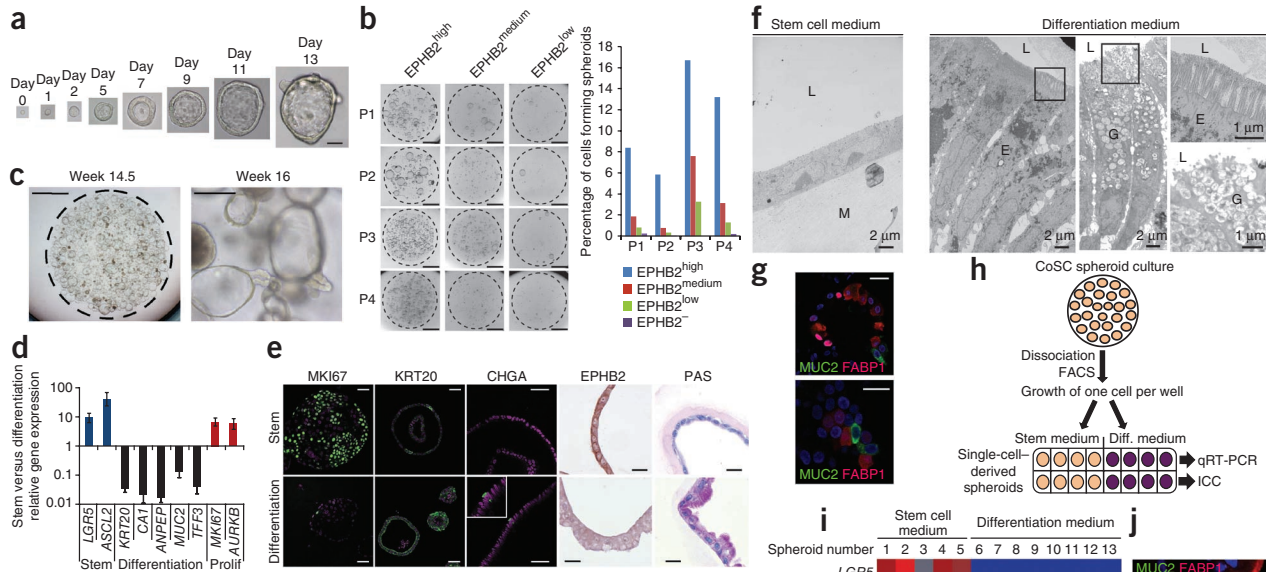


**Figure 2** Single EPHB2<sup>high</sup> human colonic crypt cells form *in vitro* spheroids with long-term proliferation and multilineage differentiation capacity. **(a)** Microscopy images documenting the growth of a representative spheroid derived from a single EPHB2<sup>high</sup> human colonic crypt cell from day 0 to day 13. Days 0–9: 40× objective, days 11–13: 20× objective. Scale bar, 50 μm. **(b)** Left, representative images of colonic spheroid cultures 2 weeks after seeding the same number of cells of each EPHB2-purified cell population. Samples were derived from four individuals suffering either from cancer (P1–P3) or from a diverticulosis (P4). Each dashed black circle represents the boundary of a Matrigel drop. Right, quantification of relative number of spheroids generated in each sample. Scale bars, 1 mm. **(c)** Microscopic images of serially passaged *in vitro* organoids derived from single EPHB2<sup>high</sup> sorted cells after more than 100 d in culture. One 50 μl Matrigel droplet is depicted (left; scale bar, 1 mm). Single spheroids maintained their microscopic appearance after 16 weeks of culture and sequential passaging (right; 10× objective; scale bar, 100 μm). **(d)** Analysis of expression of stem cell proliferation and differentiation marker genes by qRT-PCR in human colonic spheroid cultures. Data are represented as relative changes of expression between spheroids cultured in stem cell medium compared to spheroids maintained in differentiation media for 7 d. Error bars indicate s.d. (*n* = 3). **(e)** Detection of MKI67, KRT20, chromogranin A (CHGA), EPHB2 or mucrosecretory cells (periodic acid Schiff (PAS) staining) on colonic sphere cultures maintained in stem cell medium (top) or in differentiation medium over 7 d (bottom). MKI67, KRT20 and CHGA (green label) are shown as confocal images (counterstaining with DAPI in magenta), whereas EPHB2 (brown staining) was detected by immunohistochemistry (counterstaining with hematoxylin). Scale bars, 50 μm (confocal images) and 10 μm (immunohistochemistry). **(f)** Morphological features of cells obtained by EM from *in vitro*-cultured human colon organoids either cultured in stem cells or differentiation media (7 d). L, sphere lumen; M, Matrigel; E, enterocyte; G, goblet cells. Areas encompassed by squares are magnified in the right images and highlight microvilli in enterocytes and secretory granules in goblet cells. **(g)** Confocal images showing double detection of enterocytes (FABP1<sup>+</sup>) and goblet cells (MUC2<sup>+</sup>) on differentiated organoids. Counterstaining, DAPI (blue). Scale bars, 20 μm. **(h)** Schematic representation of the single-cell reseeding approach. In brief, after 6 weeks of *in vitro* culture, organoids derived from EPHB2<sup>high</sup> single cells were enzymatically and mechanically disaggregated. Organoid-derived single sorted cells were re-embedded in Matrigel and seeded in serial dilutions. Only Matrigel droplets in which one organoid regrew from a single cell were considered for further analysis. After 14 d, RNA was isolated from a subset of organoids cultured in stem medium. The rest of organoids were then cultured in differentiation medium and RNA was isolated after 5 d. **(i)** Intensity plot representing the relative gene expression of several marker genes in five single-cell–derived spheroids that were cultured in stem cell medium (1–5) and in eight single-cell–derived spheroids that underwent differentiation for 5 d (6–13). Expression was measured by qRT-PCR on mRNA extracted from each individual organoid. Numbers in color bar indicate the relative expression levels. **(j)** Confocal images showing double detection of enterocytes (FABP1<sup>+</sup>) and goblet cells (MUC2<sup>+</sup>) on differentiated organoids derived from single EPHB2<sup>high</sup> cells. Counterstaining, DAPI (blue). Scale bars, 20 μm.

from colorectal cancer or diverticulitis (**Supplementary Table 1** and **Supplementary Methods**). We selected areas of macroscopically normal mucosa that, upon histological examination, revealed no abnormalities (**Fig. 1a** and **Supplementary Fig. 1**). By FACS, we isolated crypt epithelial cell populations (epithelial cell adhesion molecule positive (EpCAM<sup>+</sup>)) expressing various surface levels of EPHB2 (**Fig. 1b**). The expression of colonic differentiation markers followed a pattern inverse to that of surface EPHB2 (**Fig. 1c**). Furthermore, EPHB2<sup>-</sup> cells showed a 150% to 2,500% reduction in expression of genes required for proliferation (**Fig. 1c**), implying that this population was largely composed of cell cycle-arrested, terminally differentiated cells. We also noticed a drift toward cells with short telomeres in populations with decreasing EPHB2 abundance (**Fig. 1d** and **Supplementary Fig. 2**).

EPHB2<sup>high</sup>, EPHB2<sup>medium</sup> and EPHB2<sup>low</sup> cell fractions represented the bottom two thirds of colonic crypts and showed equivalent expression

of cell proliferation markers, albeit MKI67 expression dropped in EPHB2<sup>low</sup> cells (**Fig. 1c**). EPHB2<sup>high</sup> cells had the longest average telomere length (**Fig. 1e**) and expressed the highest levels of mouse ISC marker mRNAs leucine-rich repeat-containing G protein-coupled receptor 5 (*LGR5*), Achaete-scute complex homolog-2 (*ASCL2*), and olfactomedin-4 (*OLFM4*)<sup>5–7</sup> (**Fig. 1c**). Expression profiling of EPHB2-purified cells (*n* = 3 mucosas) revealed a set of 90 genes whose expression was consistently higher in EPHB2<sup>high</sup> compared to EPHB2<sup>medium</sup> cells (**Supplementary Fig. 3b** and **Supplementary Tables 2** and **3**). *LGR5*, *ASCL2* and *EPHB3* as well as the catalytic subunit of telomerase reverse transcriptase (*TERT*) were included in the top positions of this gene list (**Supplementary Table 2**). AC133 surface expression or ALDEFLUOR staining, which characterize some adult stem cells, did not completely segregate CoSCs (**Supplementary Data** and **Supplementary Figs. 4** and **5**). From these data, we tentatively concluded that the EPHB2<sup>high</sup>

cell population is largely enriched in CoSCs, whereas EPHB2<sup>medium</sup> and EPHB2<sup>low</sup> cells represent transient amplifying cells at different stages of differentiation.

Recent protocols describe *in vitro* maintenance of mouse gastrointestinal organoids by reproducing ISC niche signals (such as activation of the Wnt and Notch pathways and inhibition of bone morphogenetic protein signals)<sup>5,8</sup>. We initially tested these conditions on full human colon crypts embedded in Matrigel and found that the protocol developed for mouse intestinal cells required some crucial modifications (Supplementary Methods). We observed a strict dependency on supplementation with the vitamin nicotinamide (Supplementary Fig. 6a). Furthermore, *in vitro* survival and growth of isolated crypts was potentially enhanced by addition of prostaglandin E<sub>2</sub> (PGE<sub>2</sub>), which blocks anoikis and transactivates mitogenic signaling<sup>9,10</sup> (Supplementary Fig. 6a). Under these conditions, human colonic crypts lost their upper third compartment during the first days of culture, whereas the bottom region formed closed spheroids (Supplementary Fig. 6b). These structures expanded radially through rapid cell proliferation while maintaining a central lumen. Upon mechanical dissociation and re-embedding in Matrigel, spheroids quickly re-formed closed structures that kept growing without apparent disturbance (Supplementary Fig. 6b).

Under the culture conditions developed above, single-sorted cells from human colon biopsies gave rise to spheroid-like organoids after 9–14 d (Fig. 2a and Supplementary Fig. 6c). The frequency of EPHB2<sup>high</sup> sorted cells, which grew into spheroids, varied between 6% and 17% (Fig. 2b). In all cases, decreasing EPHB2 surface abundance coincided with a lower frequency of cells capable of generating spheroids (Fig. 2b). Of note, the spheroid-forming capacity of EPHB2<sup>high</sup> cells purified from normal mucosas of individuals with either colorectal cancer or noncancerous pathologies (diverticulitis, P4 in Fig. 2b) was equivalent. Single EPHB2<sup>high</sup> cells grew exponentially (Supplementary Fig. 7) and gave rise to macroscopic spheroids (up to ~0.5 mm in diameter) within 18–21 d. Typically, we passaged them by disaggregation every week. Under this regime, EPHB2<sup>high</sup> cells could be cultured for long periods (over 4 months) in conditions of exponential growth (Fig. 2c, Supplementary Figs. 7 and 8b and data not shown). Notably, by comparative genomic hybridization analysis, we found that the genomes of cultured CoSCs remain stable (Supplementary Data and Supplementary Figs. 9 and 10).

To test the differentiation capacity of spheroids derived from EPHB2<sup>high</sup> cells, we cultured them in the absence of PGE<sub>2</sub> and Wnt3a, at the same time blocking Notch signaling by adding a  $\gamma$ -secretase inhibitor (Fig. 2d–j). This treatment led to a cease in the expression of MKI67 and upregulation of the pan-differentiation marker KRT20 (Fig. 2d,e), as well as of differentiation markers of absorptive (*ANPEP* and *CA1*) and secretory lineages (*MUC2* (mucin 2) and *TFF3* (trefoil factor 3)) (Fig. 2d). Concomitant to the onset of differentiation, the ISC program was silenced (Fig. 2d). By electron microscopy (EM), spheroids derived from EPHB2<sup>high</sup> cells appeared as a monolayer of small, nonpolarized cells displaying large, centrally positioned nuclei and no brush borders (Fig. 2f). The majority of cells were proliferating (Fig. 2e) and expressed barely detectable levels of differentiation genes (Fig. 2d,e). Notably, spheroids were enriched in the expression of stem cell markers (Fig. 2d), including high EPHB2 levels (Fig. 2e). Differentiation was accompanied by a marked morphological change that included prominent cellular polarization (Fig. 2f). EM revealed the presence of intermingled cells with either a well-defined apical brush border or large mucous vacuoles (Fig. 2f), characteristic of absorptive or mucus-secreting cells, respectively. By staining of lineage-specific

marker genes, we confirmed the emergence of a mixed population of absorptive (FABP1<sup>+</sup>) and mucus-secreting (MUC2<sup>+</sup>) cells (Fig. 2g) and also detected a low proportion (1:200 to 1:500) of enteroendocrine cells (Fig. 2e and Supplementary Fig. 11). Organoids derived from EPHB2<sup>high</sup> cells retained intact multilineage differentiation capacity even after three months in culture ( $n = 12$  passages) (Supplementary Fig. 8c). To assess multipotency, we generated single-cell-derived organoids from CoSCs that had been propagated in culture during six weeks (Fig. 2h). Approximately 6% of all cells successfully re-formed second-generation spheroids after such manipulation. They retained high expression levels of the ISC marker genes *ASCL2* and *LGR5* (Fig. 2i). Notably, upon switching to differentiation medium, all single-cell-derived spheroids analyzed ( $n = 8$ ) generated a mixed population of absorptive and mucosecreting cells (Fig. 2i,j), implying that a substantial proportion of CoSCs stay multipotent.

Collectively, these data represent what is to our knowledge the first isolation, characterization and *in vitro* expansion of a cell population largely enriched in human CoSCs. The cell culturing protocol described here allows the maintenance of an undifferentiated and multipotent ISC-like phenotype *in vitro*. Our work represents a substantial step forward toward the use of human CoSCs in regenerative medicine and toward understanding their role in pathology.

Note: Supplementary information is available on the Nature Medicine website.

#### ACKNOWLEDGMENTS

We thank Genentech for the EphB2-specific antibody Mab 2H9 and the Institute for Research in Biomedicine transcriptomic facility, electronic microscopy service (Universitat de Barcelona) and Cell separation unit (UB) for expert assistance. We thank L. Lopez Vilaro and E. Calderón Gómez for help with mucosas. This work is supported by grants to E.B. from the CONSOLIDER and Plan Nacional I+D+i Programs from Spanish Ministry of Science and Innovation (MICINN) and the European Research Council (ERC-FP7). Work was furthermore supported by grants from Instituto de Salud Carlos III FEDER (RD09/0076/00036). The 'Xarxa de Bancs de tumors' is sponsored by Pla Director d'Oncologia de Catalunya (XBTC). The M.A.B. laboratory is founded by the MICINN, the EU, the Botin and Lilly Foundations, and the Korber European Science Award to M.A.B. P.J. holds a Marie Curie Fellowship (FP7).

#### AUTHOR CONTRIBUTIONS

E.B. and P.J., study concept and design and writing of the manuscript. T.S. and H.C., development of original human colon culture method. P.J., acquisition, analysis and interpretation of data and modifications of the human CoSC culture protocol. A.M.-S. and F.M.B., profiling of human colon stem cells. D.R., bioinformatic analysis. E.S., conceptual and logistic support. M.M.G. and M.A.B., telomere length measurements. M.I., sample preparation and development of EphB2 sorting method.

#### COMPETING FINANCIAL INTERESTS

The authors declare no competing financial interests.

Published online at <http://www.nature.com/naturemedicine/>.

Reprints and permissions information is available online at <http://www.nature.com/reprints/index.html>.

- Zeki, S.S., Graham, T.A. & Wright, N.A. *Nat. Rev. Gastroenterol. Hepatol.* **8**, 90–100 (2011).
- van der Flier, L.G. & Clevers, H. *Annu. Rev. Physiol.* **71**, 241–260 (2009).
- Battle, E. *et al. Cell* **111**, 251–263 (2002).
- Merlos-Suárez, A. *et al. Cell Stem Cell* **8**, 511–524 (2011).
- Barker, N. *et al. Cell Stem Cell* **6**, 25–36 (2010).
- van der Flier, L.G. *et al. Cell* **136**, 903–912 (2009).
- van der Flier, L.G., Haeghebarth, A., Stange, D.E., van de Wetering, M. & Clevers, H. *Gastroenterology* **137**, 15–17 (2009).
- Sato, T. *et al. Nature* **459**, 262–265 (2009).
- Buchanan, F.G. & DuBois, R.N. *Cancer Cell* **9**, 6–8 (2006).
- Joseph, R.R., Yazer, E., Hanakawa, Y. & Stadnyk, A.W. *Apoptosis* **10**, 1221–1233 (2005).